23rd ABCM International Congress of Mechanical Engineering
December 6-11, 2015, Rio de Janeiro, RJ, Brazil

MODELLING AND SIMULATION OF AN ELECTRIC VEHICLE: ANALYSIS AND SOLUTIONS FOR IMPROVING MECHANICAL PERFORMANCE

Paulo Roberto Ubaldo Guazzelli
Universidade de São Paulo (USP). Av. Trabalhador São-carlense, 400. São Carlos, SP - Brazil.
paulo.ubaldo@usp.br

Marcelo Suetake
Sergio Henrique Evangelista
Osmar Ogashawara
Universidade Federal de São Carlos (UFSCar). Rod. Washington Luís, km 235, SP 310. São Carlos, SP - Brazil.
suetake@ufscar.br, toddyprof@ufscar.br, osmaroga@ufscar.br

Abstract. *Electric vehicles comprise an alternative solution for transportation in urban centers, with the advantages in reducing carbon emissions and improving air quality of cities. This fact challenges the engineering design when it must be obtained trade off solutions and substitution of ICE (Internal Combustion Engine) vehicles of a certain design category. To explore these challenges, it was made a preliminary design process of a 3 hp powertrain of 4 x 555 W dc motors vehicle to obtain guidelines to cope with or surpass the advantages of an ICE drift buggy vehicle. Changings were considered on the powertrain system and on the material structure, from steel alloy in the ICE vehicle to aluminum alloy in the electrical one. The Simulink software (MathWorks®) was used for simulation of general behavior of vehicular dynamics of both vehicle types. The analyses showed the importance of considering some design aspects as overall weight reduction, a four-speed transmission to improve performance for electrical vehicles and the problem of batteries specification and quantity. The results showed similar simulated performances for both vehicle types in terms of maximum speed and drive distance range, while the drawbacks were set on the acceleration time to reach the maximum speed.*

Keywords: *electric vehicle, mechanical performance, modelling, vehicular dynamics*

1. INTRODUCTION

Since the recent decades, researchers and companies have been keen on developing the technology of Hybrid Electric Vehicles (HEVs) and Purely Electric Vehicles (PEVs), due to a growing concern about environment, which caused more rigorous emission and fuel efficiency standards for vehicles (Ehsani *et al.*, 2010). In a multidisciplinary project, modelling and simulation of the studied system are important tools that allow for engineers to save time and resources (Bazzo and Pereira, 2003). Given that, one can highlight that mathematical modelling, where the system is represented by using differential equations, and computacional simulation, where those equations are calculated by a software, are widely used for improving vehicle design.

PEVs Tesla Roadster® and Nissan Leaf® simulated using EXCEL® by Hayes *et al.* (2011), showing good correlation of range and efficiency with published data, while the HEV Toyota Prius® was simulated in Simulink, from MATLAB®, by Sefik and Hiyama (2011). Simulink software was also used to simulate a PEV with batteries as power source in Guazzelli *et al.* (2013), where the authors avaliated the use of a manual transmission, and in Njoya *et al.* (2009), which simulated a vehicle with fuel cells.

This study aims to use modelling and simulation for improving electric conversion of a drift buggy powered by a 4.8 hp Internal Combustion Engine (ICE). Original vehicle will be simulated (considering the ICE), and an electric version will be proposed, with structural modifications in the buggy for reducing the vehicle nominal power, but maintaining mechanical performance specifications: maximum speed and driving range, that is 60 km/h and 72 km, according the manufacturer (DROPBOARDS, 2014), as well the acceleration time, that will be determined through simulation. Simulink software will be used for simulation of original ICE vehicle and proposed electric vehicle.

2. METHODS

A vehicle have propulsion and load systems, which should be considered for simulation. Regarding the ICE vehicle, three systems where modelled, as seen in Fig. 1 (a). The ICE drives the vehicle, the transmission delivers energy from ICE to the wheels and vehicular dynamics contains the opposing forces to moviment. The PEV also requires the same load models, and new propulsion models: the power source, power electronics and electric motor, according to Fig. 1 (b).

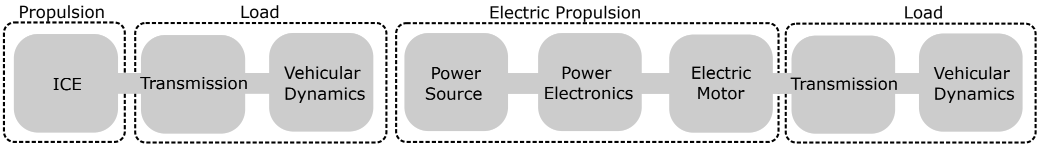

(a) ICE vehicle systems modelled (b) PEV systems modelled

Figure 1. Original and converted vehicle systems considered for simulation

2.1 Original ICE Vehicle

It is considered that a generic ICE engine behaves according to a classical relation among available torque $T_{ice}(\omega_{ice})$, power $P(\omega_{ice})$ and angular speed ω_{ice}, as in Eq. (1):

$$T_{ice}(\omega_{ice}) = \frac{P(\omega_{ice})}{\omega_{ice}} \tag{1}$$

For the case of the power, an analytical model is expressed in The Mathworks, Inc. (2015) as a product of a scale factor P_{max} (ICE maximum output power value) by an adimensional function $p(w)$, where w is the normalized factor given by $w = \frac{\omega_{ice}}{\Omega_0}$, and Ω_0 is the angular speed at which the ICE delivers maximum power. The function $p(w)$ is typically a third-order polynomial form for generic combustion engines, such that:

$$P(\omega_{ice}) = P_{max} \cdot p(w) = P_{max}\left[w(p_1 + p_2 w - p_3 w^2)\right] \tag{2}$$

The polynom $p(w)$ has three zeros, one at $w = 0$ and two others, from which one has physical meaning. By composing these above mentioned restrictions, one obtains from Eq. (1) and Eq. (2):

$$T_{ice}(w) = \frac{\delta_D P_{max}}{\Omega_0} \cdot \left(p_1 + p_2 w - p_3 w^2\right) \tag{3}$$

where it was imposed a throttle factor δ_D, ranging from 0 to 1. For generic gasoline engines, the p_1,p_2 and p_3 coefficients are equal to 1. The drift buggy uses a 160 cc ICE with maximum power of 4.8 hp at 3600 rpm, and maximum angular speed of 5500 rpm (the torque is null above this value).

The transmission is coupled to the engine, increasing torque delivery from the ICE axle ($T_{ice} = T_{in}$) to the wheels axle (T_{out}), as in Eq. (4), considering a system efficiency of η_T and an increase ratio of i, which is the relation of angular speeds in both axles of the transmission. Ratio i is constant in a simple gear, as the one in the drift buggy. Thus, a transmission with $i = 4.8$ and assumed efficiency of 90% was simulated.

$$\frac{T_{out}}{T_{in}} = \eta_T \cdot i = \eta_T \cdot \frac{\omega_{in}}{\omega_{out}} \tag{4}$$

Modelling of the forces acting during moviment is made by Eq. (5), originated from second law of Newton (Ehsani *et al.*, 2010), where the vehicle acceleration (dV_X/dt) depends of the sum of forces moving the vehicle (F_t) and resisting the moviment (F_r). Parameter M is the vehicle mass and δ is an adimensional factor for considering the effect of rotatives inertias of the system in the linear moviment.

$$\frac{dV_X}{dt} = \frac{\sum F_t - \sum F_r}{\delta M} \tag{5}$$

Three resisting forces were considered: aerodynamic, rolling and gravitacional resistances, each one a part of the right term of Eq. (6). First part is aerodynamic force, originated from air external flow around the vehicle, varying with the square of vehicle speed, where A_F is the frontal area, C_D is the aerodynamic drag coefficient, and ρ is the air density.

$$\sum F_r = \frac{1}{2}\rho C_D A_F \cdot V_X^2 + Mgf_r \cdot \cos(\beta) + Mg \cdot sen(\beta) \tag{6}$$

Rolling resistance is the second part and it models the effect produced by tires deformation. It depends of vehicle weight force (Mg), the rolling coefficient f_r and the road slope angle β. Finally, gravitacional force is modelled by the last part of Eq. (6), and is the projection of weight force on the longitudinal axis. This effect becomes a traction force during downhill.

The torque T_{out} applied in the wheels results in the main traction force F_T , as seen in Eq. (7), where R_D is the wheel radius. According to Ehsani *et al.* (2010), this force is limited during acceleration and braking, depending also on the following vehicle dimensions: Center of Gravity (CG) height h_G, distance L between axles, CG distance to front axle L_A, road and tyre μ friction coefficient. The limits are calculated as in Eq. (8).

$$\sum F_t = F_T = \frac{T_{OUT}}{R_D} \tag{7}$$

$$-\frac{\mu M g\cos(\beta)[L_A - f_r(h_G - R_D)]}{L + \mu h_G} \leq F_T \leq \frac{\mu M g\cos(\beta)[L_A - f_r(h_G - R_D)]}{L - \mu h_G} \tag{8}$$

Simulation uses parameters from Tab. 1 about the vehicular dynamics. Aerodynamic and rolling resistance coefficient were considered as in Ehsani *et al.* (2010), while friction coefficient as in Canale (1989). In addition, vehicle total mass is assumed as the sum of several components.

Table 1. Parameters used for simulation of ICE drift buggy vehicular dynamics.

Parameter	Value	Parameter	Value
ICE mass (kg)	15.0	Aerodynamic drag	0.70
Fuel mass (kg)	3.6	Wheel radius (m)	0.15
Driver mass (kg)	80.0	Rolling resistance coefficient	0.013
Structure mass (kg)	60.0	Friction coefficient	0.80
Total mass (kg)	158.6	Distance between axles (m)	1.10
Inertia factor	1.1	Distance from CG to front axle (m)	0.77
Frontal area (m^2)	0.65	CG height (m)	0.20

All the models are simulated together as in Fig. 2. ICE model produces a torque Tin, modulated by δ_D (representing the driver) and applied to input axle of transmission model, that applies a torque T_{out} in the vehicular dynamics model. This model calculates the vehicle speed V_X, as well the wheels angular speed ω_{out}. The program finally calculates the angular speed of the input axle, feeding the ICE model and closing the simulation loop.

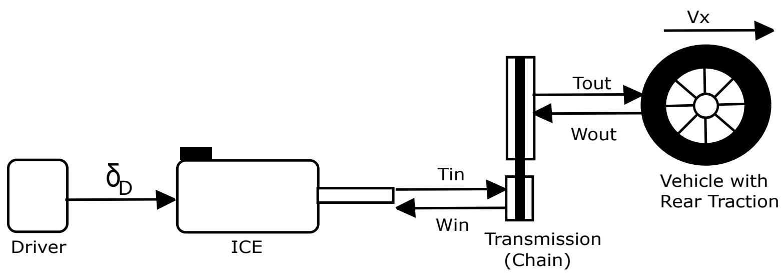

Figure 2. Complete model for ICE vehicle simulation

2.2 Proposed Electric Vehicle

A battery bank with 284 lithium cell batteries (41 branches with 7 batteries each) was considered using the model of Tremblay and Dessaint (2009), where battery is modelled as a voltage source dependent of the drained current. The battery bank data is presented in Tab. 2.

Table 2. Battery bank parameters used in simulation.

Parameter (single battery)	Value	Parameter (battery bank)	Value
Nominal voltage (V)	3.7	Nominal voltage (V)	25.9
Nominal charge (Ah)	2.2	Nominal charge (Ah)	90.2
Mass (kg)	0.051	Mass (kg)	14.6

Power electronics delivers energy from batteries to the motors. Pulse Width Modulation (PWM) is used in practice for drive the motors with a variable voltage. In this study an average value converter was modelled, producing the same mechanical performance, but allowing a faster simulation. The output voltage of the converter is given by Eq. (9), where δ_C is the converter ratio, and the current driven from batteries is calculated by Eq. (10), considering N_M motors, an efficiency η_C, assumed as 90%. The current provided has the same average profile of the one considering PWM switching, but without the ripple.

$$V_M = \delta_C \cdot V_{BAT} \tag{9}$$

$$I_{BAT} = \frac{N_M \delta_C I_M}{\eta_C} \tag{10}$$

Motor transforms electric energy into mechanical moviment, at angular speed ω_M. The permanent magnet DC motor was considered, using its dynamic model (Fitzgerald *et al.*, 2006). Armature current i_A behaves according to Eq. (11), where R_A and L_A are armature resistance and indutance, and E is the counter-electromotive force, calculated in Eq. (12), depending on rotor angular speed ω_M and the voltage constant K_E.

$$\frac{di_A}{dt} = \frac{1}{L_A}\left(V_M - R_A i_A - E\right) \tag{11}$$

$$E = K_E \omega_M \tag{12}$$

On the other hand, i_A produces an electromagnetic torque T_E according to Eq. (13), where K_T is the torque constant, numerically equal to the voltage constant. Equation (14) then determines the torque T_M effectively produced in the motor axle, considering mechanical losses, where J is the motor inertia, B is the viscous friction coeffcient and F is the Coulomb friction torque.

$$T_E = K_T i_A \tag{13}$$

$$T_M = N_M \left(T_E - J\frac{d\omega_M}{dt} - B\omega_M - F\right) \tag{14}$$

Four 555 W electric motors with nominal angular speed of 3300 rpm and nominal current of 32 A each are considered for the drift buggy. Experimental tests obtained the parameters of Tab. 3, used in simulation.

Table 3. Electric motor obtained parameters for simulation.

Parameter	Value	Parameter	Value
Armature resistance (Ω)	0.126	Inertia (km.m^2)	0.00012493
Armature inductance (H)	0.00007265	Viscous friction coefficient (Nm.s/rad)	0.075229
Voltage constant (V.s/rad)	0.05915	Coulomb friction torque (Nm)	0.0015

A control strategy is necessary to keep electric motor current under the nominal value (32 A). The strategy acts modifying converter ratio, controlling the angular speed and electric current. A cascaded topology was used, according to Castrucci *et al.* (2011), using two Proporcional-Integral controllers (PI), as can be seen in Fig. 3. The angular speed control loop has angular speed reference as input (the driver comand), as well the measured motor angular speed. Current reference is the output of this loop, feeding the current control loop, that determines the required ratio to the converter (value limited between 0 and 1). Both measured angular speed and current were normalized by nominal values (3300 rpm and 32 A, respectively).

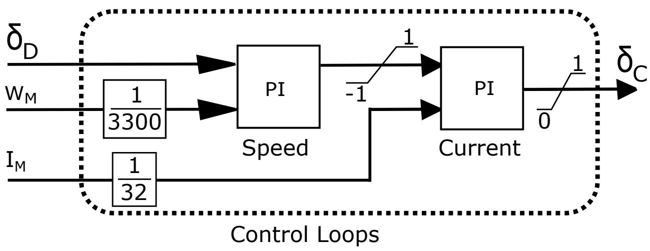

Figure 3. Control loops developed for the PEV

The complete PEV model can be seen in Fig. 4. As in the ICE model, it is a loop calculation. The driver provides a reference for the control loops, that calculates the converter ratio δ_C. The batteries voltage is modulated and applied in the motor, that produces torque, simulating the vehicle as the ICE one. Addicionally, the motor model calculates the drained current, which causes a drained current in the batteries, closing the electrical loop as well.

The same models of transmission and vehicular dynamics were used for the PEV. However, some parameters were changed in order to improve PEV performance. Since the electric motor has a lower nominal angular speed, transmission ratio i must be lower. Regarding the vehicle structure, one can reduce its weight by changing its material specification. Aluminum alloy has a density almost three times lower than steel (used in the drift buggy), so a structure with half of original mass was considered to permit some weight reduction and some design adjustments in order to fulfil the mechanical needs of stiffness and resistance. The calculation of total mass also changes, considering batteries and electronics. Table 4 resumes applied modifications .

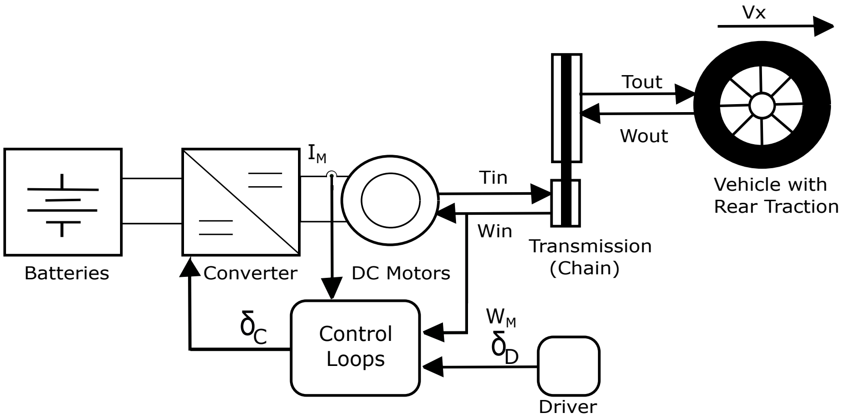

Figure 4. Complete model for PEV simulation

Table 4. Modifications in load models for PEV simulation.

Parameter	Value	Parameter	Value
Mass of four motors (kg)	13.6	Aluminium structure mass (kg)	30.0
Batteries mass (kg)	14.6	New total mass (kg)	139.2
Power electronics mass (kg)	1.0	Transmission ratio i	3.1

According to Guazzelli *et al.* (2013), is possible to improve vehcile performance by adding transmission stages in the gearbox, compared to a single speed transmission. Therefore, a four-speed transmission were also considered. The i ratio used in Eq. (4) can assume four values, instead of one, according a lookup table function of vehicle speed, as can be seen in the model of Fig. 5, which replaces the single speed transmission model used in Fig 4. Table 5 shows the ratios used, as well the speeds where each change of ratio occurs and the adicional mass considered for the transmission.

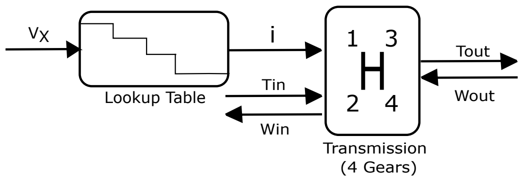

Figure 5. Model of four-speed transmission

Table 5. Parameters for the four-speed transmission.

Parameter	Value	Parameter	Value
Ratios	7.5/4.8/3.9/3.1	Speeds for change (km/h)	22/36/45
Transmission mass budget (kg)	10.0	New total mass (kg)	149.2

2.3 Calculation of Driving Range

The PEV dynamic simulation provides its acceleration time (by analysing the speed profile), as well the maximum speed. For obtaining the driving range, the profiles of vehicle speed and batteries current were postprocessed. Assuming a simulation time T_{sim}, current profile $i_{bat}(t)$ with final current I_F and speed profile $v_X(t)$ with final speed V_{X_F}, Eq. (15) obtains the vehicle duration time T_D in seconds, used in Eq. (16) for calculation of the driving range S in meters. Batteries nominal charge Q_{bat} is given in Ah. The numerical integrals were calculated using the trapezoidal method.

$$T_D = \frac{1}{I_F}\left(3600 Q_{bat} - \int_0^{T_{sim}} i_B(t)dt\right) + T_{sim} \tag{15}$$

$$S = (T_D - T_{sim}) V_{X_F} + \int_0^{T_{sim}} v_X(t)dt \tag{16}$$

3. RESULTS AND DISCUSSIONS

The ICE vehicle (ICEV), PEV with single speed transmission (PEV1s) and PEV with four-speed transmission (PEV4s) were simulated in Simulink with $T_{sim} = 40$ s on a flat road ($\beta = 0°$), using fixed step size of 1 ms, and the ode3 solver of MATLAB® (Bogacki-Shampine integration method).

The rotor and vehicle speeds obtained in the simulations are presented in Fig 6. Figure 6 (a) shows that ICE reached 5200 rpm, near its maximum speed, while the electric motors reached their nominal speed of 3300 rpm. The four speed transmission allowed the electric motor to operate closer to its nominal speed during acceleration. Given the different ratio transmissions, the three vehicles reached almost the same speed, as seen in Fig. 6 (b). Regarding the acceleration time, the ICE vehicle presented a better performance, and the PEV with four-speed transmission had a improved performance compared to the single speed one.

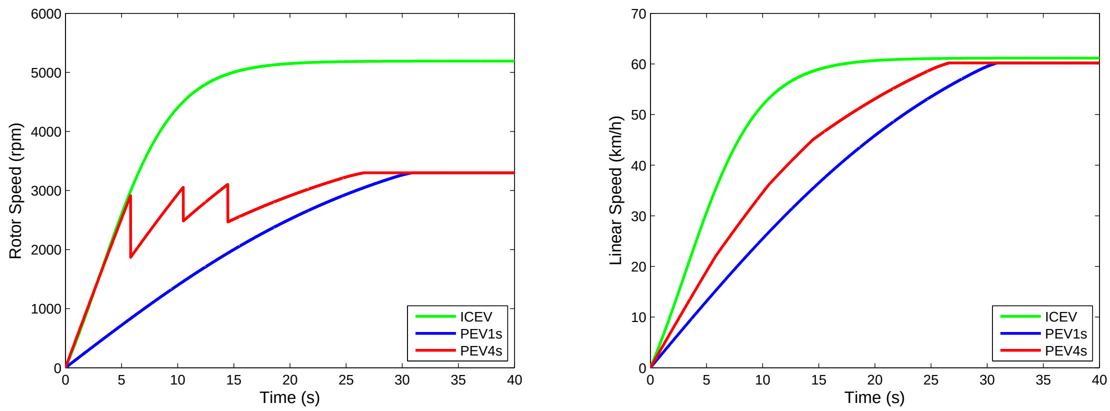

(a) ICE and electric motors rotor speed (b) Vehicles speed

Figure 6. Mechanical performances obtained in simulations

Regarding the PEVs simulated, Fig. 7 (a) shows that motors currents were limited by the controllers under 32 A during the acceleration. Calculation of driving range uses the batteries current profile, showed in Fig. 7 (b). PEV with single speed transmission presents a current peak at the end of acceleration, and a stationary lower value at the end. The PEV with four-speed transmission also presents current peaks at each ratio change, however, the lower stationary value is reached earlier.

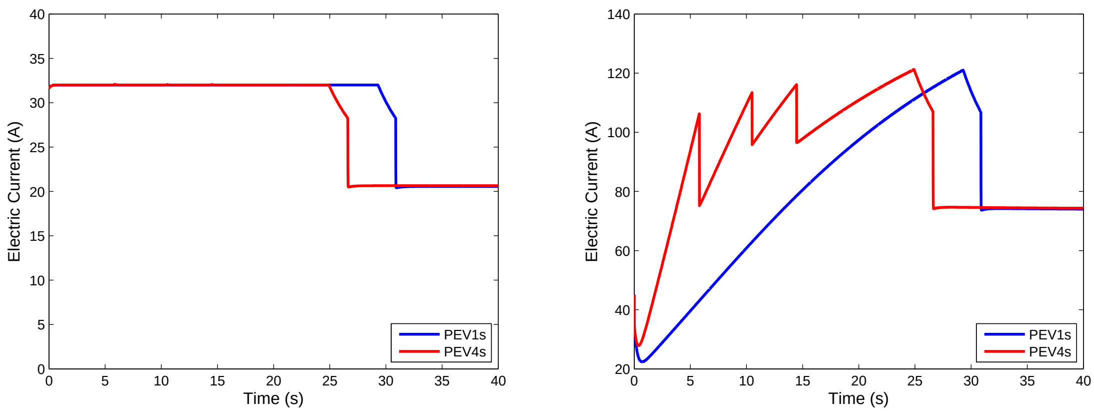

(a) Electric motors current (b) Battery bank current

Figure 7. Currents profiles obtained in PEVs simulations

Table 6 summarizes the analysed performances. It can be seen that analysed PEVs were able to perform similar maximum speed and driving range, when compared to the original ICE vehicle. ICE vehicle developed a higher acceleration, because of the powertrain with higher power (4.8 hp, against less than 3 hp), but the new four-speed transmission considered was able to improve PEV performance, showing one alternative to enhance performance without increase of the powertrain nominal power.

Table 6. Performance parameters of simulated vehicles.

Parameter	ICEV	PEV1s	PEV4s
Maximum speed (km/h)	61.2	60.2	60.2
Driving range (km)	72.0	73.1	72.7
Acceleration time (s)	17.1	30.9	26.5

4. CONCLUSIONS

Simulation of an ICE vehicle and two PEVs in Simulink showed that ICE parameters were equivalent to manufacturer data, while the proposed PEV with fixed speed transmission performed the same maximum speed and driving range, but with a larger acceleration time, due to the lower nominal power used. The use of a transmission with four gears was proposed, improving the PEV acceleration time, showing that mechanical changes in the project can help to compensate the power difference between ICE vehicle and PEV. The replacement of steel structure for a aluminium one is also a possibility to increase performance.

In future works, results obtained in simulations must be verified by experimental tests performed in the drift buggy after the powertrain conversion. In addition, one can highlight the optimization of transmission ratios, improving the PEV performance, and also the use of a continuously variable transmission, obtaining an optimized function for the ratio i. The present methodology of modelling and simulation can also be extended for use in others PEV projects.

5. ACKNOWLEDGEMENTS

The authors thank to CNPq for financial support with public notice MCTI/CNPq/SPM-PR/Petrobras n^o 18/2013.

6. REFERENCES

Bazzo, W.A. and Pereira, L.T.d.V., 2003. *Introdução a Engenharia: Conceitos, Ferrramentas e Comportamentos*. Editora da UFSC, 2nd edition.

Canale, A.C., 1989. *Automobilística: Dinâmica e Desempenho*. Érica, São Paulo.

Castrucci, P.L., Bittar, A. and Salles, R.M., 2011. *Controle Automático*. LTC.

DROPBOARDS, 2014. *Manual do Usuário Drift Buggy 160 cc*. DROPBOARDS. URL `http://dropboards.com.br/manual-de-instrucao/`.

Ehsani, M., Gao, Y. and Emadi, A., 2010. *Modern Electric, Hybrid Electric, and Fuel Cell Vehicles: Fundaments, Theory, and Design, Second Edition*. CRC Press, Boca Raton, 2nd edition. ISBN 9781420053982.

Fitzgerald, A.E., Kingsley, Jr, C. and Umans, S.D., 2006. *Máquinas Elétricas com Inrodução à Eletrônica de Potência*. Bookman, 6th edition.

Guazzelli, P.R.U., Suetake, M., De Francisco, C.A. and Ogashawara, O., 2013. "Proposta e Simulação de Controle de Motor CC para Veículos Elétricos Considerando a Dinâmica Veicular". In *Proceeding Series of the Brazilian Society of Computational and Applied Mathematics*. Vol. 1. doi:10.5540/03.2013.001.01.0055.

Hayes, J.G., de Oliveira, R.P.R., Vaughan, S. and Egan, M.G., 2011. "Simplified Electric Vehicle Power Train Models and Range Estimation". In *2011 IEEE Vehicle Power and Propulsion Conference*. IEEE, pp. 1–5. ISBN 978-1-61284-248-6. doi:10.1109/VPPC.2011.6043163.

Njoya, S., Tremblay, O. and Dessaint, L.a., 2009. "A Generic Fuel Cell Model for the Simulation of Fuel Cell Vehicles". In *2009 IEEE Vehicle Power and Propulsion Conference*. IEEE, pp. 1722–1729. ISBN 978-1-4244-2600-3. doi: 10.1109/VPPC.2009.5289692.

Sefik, I. and Hiyama, T., 2011. "Performance evaluation of hybrid powertrain system simulation model for Toyota Prius car". In *International Aegean Conference on Electrical Machines and Power Electronics and Electromotion, Joint Conference*. IEEE, September, pp. 404–407. ISBN 978-1-4673-5003-7. doi:10.1109/ACEMP.2011.6490632.

The Mathworks, Inc., 2015. *Gasoline Engine*. The Mathworks, Inc. URL `http://www.mathworks.com/help/physmod/sdl/drive/gasolineengine.html`.

Tremblay, O. and Dessaint, L.a., 2009. "Experimental Validation of a Battery Dynamic Model for EV Applications". *World Electric Vehicle Journal*, Vol. 3, pp. 1–10.

7. RESPONSIBILITY NOTICE

The authors are the only responsible for the printed material included in this paper.